Biomass Conversion and Biorefinery (2023) 13:4241–4253
https://doi.org/10.1007/s13399-021-02219-w

ORIGINAL ARTICLE

Structural-based analysis of antibacterial activities of acid condensate from palm kernel shell

Mohd Amir Asyraf Mohd Hamzah[1] · Rosnani Hasham[1] · Nik Ahmad Nizam Nik Malek[2] · Raja Safazliana Raja Sulong[1] · Maizatulakmal Yahayu[3] · Fazira Ilyana Abdul Razak[4] · Zainul Akmar Zakaria[1]

Received: 14 August 2021 / Revised: 23 November 2021 / Accepted: 9 December 2021 / Published online: 18 January 2022

Abstract

Acid condensate (AC) is reported to exhibit various biological activities including antimicrobial, antioxidant, and anti-inflammatory that are valuable in assisting wound healing process. In this study, concentrated AC extract (CACE) obtained from microwave-assisted pyrolysis of palm kernel shells (PKS) was fractionated where fractions with similar profiles were pooled into combined fractions of acid condensate (CFACs). CACE and CFACs were evaluated for their total phenolic content, antioxidant activities, and antibacterial activity towards *Escherichia coli*, *Pseudomonas aeruginosa*, *Staphylococcus aureus*, and *Enterococcus faecalis*. The antibacterial mode of action of CFAC 3 compounds was evaluated by its binding energy and physical bond formation towards bacterial DNA gyrase (PDB ID: 4DUH) and tyrosyl-tRNA synthetase (PDB ID: 1JIJ) using molecular docking software AutoDock Vina. A total of 134 fractions were obtained and pooled into 9 combined fractions (CFAC 1–9). CFAC 3 had the highest total phenolic content (624.98 ± 8.70 µg gallic acid/mg of sample) that accounted for its highest antioxidant activities (1247.13 ± 27.89 µg Trolox/mg sample for ABTS assay and 24.26 ± 0.71 mmol Fe(II)/mg sample for ferric reducing antioxidant power, FRAP). Gas chromatography–mass spectrometry (GC–MS) revealed phenol and its derivatives as the major compounds in CFAC 3. CFAC 3 exhibited highest antibacterial activities against all tested bacteria particularly against *S. aureus* with minimum inhibitory concentration (MIC) of 0.10 mg/mL and minimum bactericidal concentration (MBC) of 0.33 ± 0.11 mg/mL. Molecular docking analysis suggested favorable binding energy for all chemical compounds present in CFAC 3, notably 1-butanone, 3-methyl-1-(2,4,6-trihydroxy-3-methylphenyl) towards the DNA gyrase (-6.9 kcal/mol), and tyrosyl-tRNA synthetase (− 7.5 kcal/ mol) enzymes. To conclude, CFAC 3 from PKS has the potential to be used as an alternative antibacterial agent which is biodegradable and a more sustainable supply of raw materials.

Keywords Acid condensate · Antioxidant · Antibacterial · Molecular docking · Palm kernel shell

Highlights
- CFAC 2 and CFAC 3 showed higher total phenolic content and antioxidant activity compared to CACE.
- GC–MS analysis showed phenolic compounds were successfully concentrated in the CFAC 1–3.
- CFAC 3 exhibited enhanced good antibacterial activity compared to CACE.
- Molecular docking analysis supported the antibacterial properties of phenolic compounds present in CFAC 3.

✉ Zainul Akmar Zakaria
zainulakmar@utm.my

[1] School of Chemical and Energy Engineering, Faculty of Engineering, Universiti Teknologi Malaysia, 81310 Johor Bahru, Johor, Malaysia

[2] Department of Biosciences, Faculty of Science, Universiti Teknologi Malaysia, 81310 Johor Bahru, Johor, Malaysia

[3] Institute of Bioproduct Development, Universiti Teknologi Malaysia, 81310 Johor Bahru, Johor, Malaysia

[4] Department of Chemistry, Faculty of Science, Universiti Teknologi Malaysia, 81310 Johor Bahru, Johor, Malaysia

1 Introduction

By 2020, Malaysia was expected to generate over 80 million tonnes of solid oil palm biomass such as empty fruit bunches, palm kernel shell (PKS), oil palm fronds, and mesocarp fiber [1]. Several green approaches are highly considered to treat oil palm biomass including using

thermal-conversion method such as microwave-assisted pyrolysis. Microwave-assisted pyrolysis is an advanced fast pyrolysis technique that applies electromagnetic irradiation for rapid heating from within of the materials in the absence of oxygen which gives higher yield of acid condensate and biogas in a relatively shorter residence time [2].

Acid condensate (AC), also known as wood vinegar, is an acidic (pH around 2.5 to 3.5) reddish-brown aqueous liquid obtained from the condensation of volatile matters generated during the pyrolysis process. AC consists of many valuable organic compounds such as phenol and derivatives, aldehydes, ketones, pyran and furan derivatives, and polyphenolic compounds [3]. PKS has been the subject of interest due to its high amount of lignin content which correlates to the yield of phenolic compounds [4] that is responsible to the high antioxidant properties of AC and antibacterial activity [5].

Uncontrolled growth and its resistance development of bacteria and fungi have been a major concern in agricultural, environment, human, and animal health since its presence resulted in human, animal, and plant diseases and low yielding production quality [6]. Currently, suitable antimicrobial topical treatment comprises of antiseptics and antibiotics whereas commercial antiseptics based on silver, biguanide, iodine, chlorine, and hydrogen peroxide have been reported to exhibit cytotoxicity to host cells [7]. In view of this, natural antimicrobial agents such as curcumin and aloe vera can be safer replacement as they exhibit low cytotoxicity [8]. AC offers a promising alternative for antibiotic, antiseptic, and chemicals for treatment of human and plant against microbiological infections/attacks as AC exhibits antibacterial [9], antifungal [9], anti-inflammatory [10], herbicide [11], and antibiotic in poultry [12]. In addition, AC is considered low cytotoxic at 100-fold dilution [13] and does not pose severe hazard to the environment [14].

Mechanisms of antibacterial action of phenol and its derivatives, which is main functional groups of AC, have been reported to be mainly associated to the disruption of cytoplasmic membrane permeability causing the efflux of ions as their primary mode of antibacterial action [15]. However, there are some reports in which the phenolic derivatives are also able to inhibit cell wall synthesis, protein synthesis, and DNA synthesis through binding interaction with enzymes, DNA, or molecules associated to bacterial growth [16]. One of those includes the inhibition of tyrosyl-tRNA synthetase. It belongs to the aminoacyl-tRNA synthetases (aaRSs) and is responsible for catalyzing the covalent binding of amino acids to their respective tRNA to form charged tRNA during protein biosynthesis process. Topoisomerase II DNA gyrase, which is exclusive for bacteria, is an enzyme that can introduce negative supercoils into DNA by ATP consumption [17]. To screen and elucidate the inhibitory ability of phenolic compounds by binding the target DNA or enzymes, computational tools such as molecular docking is preferred as a faster and less costly methods compared to experimental approach. Molecular docking allows for characterization of the behavior of small molecules in the binding site of the target protein as well as elucidating fundamental biochemical processes [18] before further validated using experimental approach.

This work focused on evaluation of the antioxidant, antibacterial activities, and antibacterial mode of action of combined fractions of optimized AC extract against common pathogenic *Escherichia coli* (*E. coli*), *Pseudomonas aeruginosa* (*P. aeruginosa*), *Staphylococcus aureus* (*S. aureus*), and *Enterococcus faecalis* (*E. faecalis*). It also worthy to note that this is also the first report on the use of molecular docking approach to determine molecular interaction between AC compounds with target enzymes associated to bacterial activity.

2 Materials and methods

2.1 Production, extraction, and fractionation of AC

PKS was obtained from one oil palm mill located in Kluang, Johor, Malaysia. It was washed, sun-dried, and stored at room temperature prior to use. The production of AC from PKS using laboratory-scale microwave-assisted pyrolysis reactor was as described previously [19]. In general, optimized parameters to produce AC containing highest concentration of phenolic compounds were as follows: microwave power of 580 W, nitrogen flow rate of 2.4 L/min, and final temperature of 480 °C. AC was extracted using 99.5% ethyl acetate, concentrated using rotary evaporator (Heidolph, Laborota 4003, Germany) and termed as concentrated AC extract (CACE). The CACE was fractionated using a column chromatography (5 cm i.d. × 80 cm) and silica gel (0.063–0.200 mm, Merck, Germany) as stationary phase, with moving-phase consisting of increasing polarity of solvent system of *n*-hexane, ethyl acetate, and methanol (QRec). The collected 134 different fractions collected were pooled into 9 final fractions (termed as CFAC 1–9) based on similarity of thin layer chromatography profile. Fractions 10–11 (CFAC 1), fractions 12–16 (CFAC 2), fractions 17–24 (CFAC 3), fractions 25–32 (CFAC 4), and fractions 33–40 (CFAC 5) were pooled and highlighted.

2.2 Total phenolic content and antioxidant activity

The total phenolic content (TPC) in AC was determined as follows [20]: 1 mL of the AC extract or fraction and 1 mL of 50% of Folin–Ciocalteu reagent (Merck, Germany) were mixed in 10 mL test tube followed by the addition of 1 mL of 10% sodium carbonate (105.99 g/mol, QRec, New Zealand).

The mixture was left to stand for 2 h at room temperature and the absorbance was measured at 765 nm using UV–vis spectrophotometer (Shimadzu UV-1800, Japan). Similar procedures were repeated for gallic acid (Merck, Germany) that acted as standard. TPC determined was expressed as µg gallic acid equivalent/ mL of dried sample (µg/mL). The 2,2-diphenyl-1-picrylhydrazyl (DPPH, Aldrich, Germany) assay was performed with slight modification to the method of Brand-Williams et al. [21] where 1 mL of CACE or CFACs was mixed with 2 mL of methanolic DPPH reagent in a 10 mL test tube. The mixture was shaken at 100 rpm and allowed to stand for 30 min at room temperature. The absorbance was measured at 517 nm with methanol as blank. Ferric reducing antioxidant power (FRAP) assay was conducted according to Ma et al. [20] by adding 100 µL of 30 µg/mL AC samples or standard L(+)-ascorbic acid (QRec, New Zealand) and butylated hydroxyanisole, 96% (BHA, Acros Organics, Belgium) respectively into 3 mL of freshly mixed FRAP reagent (300 mM acetate buffer (pH 3.6), 10 mM 2,4,6-tripyridyl-s-triazine (TPTZ, Acros Organics, Belgium) dissolved in 40 mM hydrochloric acid (QRec, New Zealand), and 20 mM ferric chloride (Merck, Germany) in the ratio of 10:1:1 and shaken thoroughly before being left upright to react for 90 min at 37 °C in the dark. The absorbance of the mixture was recorded at 593 nm using UV–vis spectrophotometer. The results were expressed as mmol Fe(II) being reduced by per milligram of sample (mmol Fe(II)/mg sample). 2,2′-Azino-bis(3-ethylbenzothiazoline-6-sulfonic acid (ABTS) assay was carried out as performed by Re et al. [22]. ABTS radical cation was prepared by mixing both 7 mM ABTS (Merck, Germany) solution and 4.9 mM potassium persulfate (Sigma-Aldrich) solution in 1:1 ratio (v/v). The radical stock solution of ABTS•+ was diluted using ethanol to an absorbance of 0.8 ± 0.005 at 734 nm. Trolox (Aldrich, Germany) solution was used to generate Trolox standard curve. Samples or standards (L(+)-ascorbic acid and butylated hydroxyanisole) with volume of 0.4 mL (20 µg/mL) were mixed with 3.6 mL of the ABTS•+ solution and incubated at 37 °C for 7 min followed by measurement at 734 nm.

2.3 Chemical composition analysis

Qualitative chemical composition analysis of AC was determined using gas chromatograph-mass spectrometer (GC–MS, Agilent 7890B GC/MS System with 5977B MSD, USA) based on the method suggested by Zhai et al. with slight modification [23]. About 1 µL of filtered sample (CACE, CFAC 1, CFAC 2, and CFAC 3) was injected with a split rate of 20:1 into the capillary column (Agilent HP-5 ms Ultra Inert) with diameter of $30\ m \times 0.25$ mm. The injector pressure and split flow rate were 10.97 psi and 23.8 mL/min respectively. Helium gas was used as a carrier gas at a flow rate of 2 mL/min and the temperature of injector was at 300 °C for 37 min. As for mass spectrometry (MS), the electron ionization with 70 eV was used to detect the mass fragment at scan range between 50 to 550 m/*z*. The ion source temperature and transfer line have been set at 200 °C and 300 °C respectively. The GC peak areas were integrated, and the component identification was done by comparing the MS with standards and with a library search (National Institute of Standard and Technology (NIST), USA).

The infrared spectra of the analyzed sample were measured using Frontier Fourier-transform infrared spectroscopy (FTIR) spectrometer (Perkin-Elmer, USA) equipped with an universal attenuated total reflection (UATR) accessory with diamond crystal at room temperature. Sixteen scans were registered during the measurement, and subsequently, the program averaged the results for all spectra. Spectral transmittance measurements were recorded in the region from 650 to 4000 cm^{-1} at a resolution of 2 cm^{-1}.

2.4 Antibacterial activity

The bacterial strains used in this study were *Staphylococcus aureus* (ATCC 6538), *Enterococcus faecalis* (ATCC 29,212), *Pseudomonas aeruginosa* (ATCC 15,442), and *Escherichia coli* (ATCC 11,229) which were obtained from the culture collection of Nanomaterial Lab 1, Department of Biosciences, Universiti Teknologi Malaysia. Bacterial suspension was prepared by inoculating single colony bacteria into 5 mL of sterile saline water until the turbidity of the bacterial suspension reached 0.5 McFarland standard solution. Disk inhibitory assay was carried out using method described by Hudzicki [24]. Sterilized commercial disk (Whatman, England) with a diameter of 6.0 mm was added with 30 µL of CACE or CFAC 1–3 (100 mg/mL). Commercial disks impregnated with kanamycin (30 µg/mL, Chemcruz, USA) and methanol were used as positive and negative control, respectively. The prepared bacterial suspension was inoculated onto Muller-Hinton (MH) agar (Merck, Germany). The prepared disks were aseptically transferred onto the surface of the agar plate. The agar plate was incubated at 37 °C for 24 h. The antibacterial activity was determined by measuring the diameter of the inhibition zones forming around the disk.

The 96-well microdilution assay for minimum inhibitory concentration (MIC) determination was carried out as based on previous method with some modifications [25, 26]. One hundred microliters of MH broth (Merck, Germany) was transferred into each of the 96-wells of the microtiter plate. One hundred microliters of sample (100 mg/mL) in 50% v/v methanol was added into the first column of the plate. After mixing, 100 µL of the mixture was pipetted into the second column (twofold dilution) and mixed. The procedure was repeated until the eleventh column. The twelfth column was

left for sterility control. Twenty microliters of the prepared bacterial suspension was pipetted into all wells. Final concentration of samples (CACE and CFAC 1–3) and antibiotics (kanamycin) ranged from 0.049 mg/mL to 50 mg/mL and from 0.19 µg/mL to 200 µg/mL, respectively. The 96-well plates were incubated (Memmert, German) at 37 °C for 24 h. The resazurin (0.015%w/v, Sigma-Aldrich, Germany) was added to all wells (30 µl per well), and further incubated for 2–4 h for the observation of color change. Minimum bactericidal concentration (MBC) is the lowest concentration of AC samples able to kill the bacterium. MBC was performed directly after MIC test. An aliquot of 20 µL of bacterial suspension was inoculated on MH agar using 20 µL pipette prior to incubation at 35 °C for 24 h. MBC was determined at concentration where there was no bacterial growth exhibited. The result was expressed as means of triplicate experiments.

2.5 Molecular docking studies

Preparation of ligands was carried out using the same procedure as described by Rabiu et al. [10]. The 3D chemical structures of major chemical compounds in CFAC 3 were extracted from PubChem and underwent energy minimization using density functional theory (DFT) (B3LYP) method. The X-ray crystal structures of bacterial DNA gyrase (PDB ID: 4DUH) and tyrosyl-tRNA synthetase (PDB ID: 1JIJ) were retrieved from Protein Data Bank (www.pdb.org) and prepared as macromolecules for docking using AutoDockTools 1.5.6. Water molecules and ligands were removed, all non-polar hydrogens were merged (removed), and partial atomic charges were assigned using the Gasteiger-Marsili method. The enzymes were prepared as PDBQT files and kept as a rigid structure for molecular docking.

AutoDock Vina [27] was used to simulate docking interaction and evaluate possible binding mode between CFAC 3 compounds towards bacterial DNA gyrase, and tyrosyl-tRNA synthetase. Configuration files were created for both the proteins by setting suitable Cartesian coordinates to generate grid box. The ligand inhibitor compound was extracted from the PDB crystal structure and docked again as a self-validation method. For *E. coli* DNA gyrase 4DUH, the procedure used was similar to Ghannam et al. with coordinates for *X*, *Y*, and *Z* axis which were − 7.434, 24.85, and − 0.94, respectively, and dimensions for grid box were 18 × 18 × 18 A° [28]. For *S.* aureus tyrosyl-tRNA synthetase, the procedure used was similar to Pisano et al. with coordinates for *X*, *Y*, and *Z* axis which were − 13.004, 13.539, and 84.405, respectively, and dimensions for grid box were 14 × 14 × 14 A° [17]. Ten best poses were generated for each ligand and scored using AutoDock Vina scoring functions. Based on the docked energy, all the ligands were ranked. The docked complex forming hydrogen bond (H bond) and other parameters like intermolecular energy (kcal/mol) was analyzed by BIOVIA Discovery Studio Visualizer v19.1.0.18287.

2.6 Statistical analysis

Quantitative data were analyzed using Microsoft Office Excel, GraphPad Prism 7.0 (GraphPad Software, Inc.) and all the results were expressed as a mean ± standard deviation.

3 Results and discussion

3.1 Total phenolic content and antioxidant activity

The total phenolic content and antioxidant activity of CACE and CFACs obtained are as tabulated in Table 1. CFAC 3 exhibited the highest TPC of 624.98 ± 8.70 µg gallic acid/mg of sample followed by CFAC 1, CFAC 2, and CACE which showed 434.02 ± 2.14, 343.80 ± 15.19, and 296.13 ± 6.26 µg gallic acid/mg of sample, respectively. The subsequent CFACs also exhibited relatively high amount TPC but lower as compared to CACE. CFAC 1–3 showed higher TPC content values compared to the CACE which aligned to the many reports that observed the trend of fraction to

Table 1 Total phenolic content and antioxidant activity of CACE and CFACs

Antioxidant assay	TPC (µg gallic acid/mg sample)	DPPH, IC_{50} (µg/mL)	ABTS (µg Trolox/mg sample)	FRAP (mmol Fe(II)/mg sample)
CACE	296.13 ± 6.26	81.76 ± 2.81	816.95 ± 30.49	9.22 ± 0.66
CFAC 1	343.80 ± 15.19	94.64 ± 8.06	1098.99 ± 17.75	10.63 ± 0.39
CFAC 2	434.02 ± 2.14	27.55 ± 2.70	1118.10 ± 22.89	15.24 ± 0.80
CFAC 3	624.98 ± 8.70	29.47 ± 0.74	1247.13 ± 27.89	24.26 ± 0.71
CFAC 4	228.48 ± 2.66	98.92 ± 16.62	556.61 ± 10.78	10.33 ± 0.28
CFAC 5	229.40 ± 2.37	130.93 ± 26.44	634.77 ± 15.33	8.56 ± 0.31
BHA	-	29.63 ± 1.16	1575 ± 40.07	13.17 ± 0.18
Ascorbic Acid	-	36.62 ± 1.34	148.99 ± 1.34	7.68 ± 0.17

have higher TPC than the plant extract [29, 30]. Most of the phenolic compounds were eluted early due to the moderate polarity solvent system of *n*-hexane–ethyl acetate which had a good elution effect on monophenols and derivatives [31, 32]. High amount of TPC in the CACE was due to high lignin content as phenol and derivatives were mainly generated from thermal degradation of lignin content which is very high in PKS [33]. The obtained TPC value of CACE was better that AC obtained from oil palm fiber [34] and pineapple waste biomass (9.50 ± 0.11) [35].

CACE exhibited lower DPPH radical scavenging activity as compared to ascorbic acid and BHA as its IC_{50} value of 81.76 ± 2.81 µg/mL was double the IC_{50} values of both standards. However, the CFAC 2 and CFAC 3 with IC_{50} of 27.55 ± 2.63 µg/mL and 29.47 ± 0.74 µg/mL, respectively, exhibited better or similar radical scavenging activity than both standards ascorbic acid and BHA. CFAC 2 has lower IC_{50} value than CFAC 3 which was due to the nature and number of functional group available in the fraction compounds for antioxidant reaction as catechol (CFAC 2) has two hydroxyl group compared to one hydroxyl group in syringol (CFAC 3) [36]. The rest of the CFACs revealed weaker antioxidant activity as CACE as the IC_{50} values were much larger. High DPPH activity of AC also has been reported from walnut [37], rice hull [38], and *Litchi chinensis* which exhibited higher TPC than ascorbic acid [39].

CACE and CFACs exhibited higher ABTS radical scavenging values than ascorbic acid (148.99 ± 1.34 µg Trolox/mg sample) but lower than BHA (1575 ± 40.07 µg Trolox/mg sample). BHA has higher ABTS scavenging ability due to the presence of large substituents on the aromatic ring which reduces the capability of free radicals to dimerize with the phenolic hydroxy group by steric crowding, thereby increasing the likelihood of hydrogen atom transfer [40]. CFAC 3 displayed the highest ABTS radical scavenging activity was 1247.13 ± 27.89 µg Trolox/mg sample, followed by CFAC 2 (1118.10 ± 22.89 µg Trolox/mg sample) and CFAC 1 (1098.99 ± 17.75 µg Trolox/mg sample). These CFACs showed higher ABTS radical scavenging activity as compared to CACE probably due to higher concentration of phenolic compounds in the sample. The descending order of ABTS cation radical scavenging activity is BHA > CFAC 3 > CFAC 2 > CFAC 1 > ascorbic acid. Monophenolic compounds which are majorly found in the AC have been reported to scavenge ABTS + • through the donation of hydrogen atom, as well as through electron transfer or by a combination of the two mechanisms [41, 42].

CFAC 3 displayed the highest reducing ability towards TPTZ-Fe (III) with FRAP value 24.26 ± 0.71 mmol Fe(II)/mg sample, followed by CFAC 2 (15.24 ± 0.80 mmol Fe(II)/mg sample) and BHA (13.17 ± 0.18 mmol Fe(II)/mg sample) as shown in Table 1. CFAC 3 and CFAC 2 have higher antioxidant activity than both standards ascorbic acid and BHA. CACE showed FRAP value of 9.22 ± 0.66 mmol Fe(II)/mg sample which was higher than standard ascorbic acid (7.68 ± 0.17) but lower than BHA. Overall, these findings also showed that the correlation between TPC and antioxidant activity could be due to the phenolic compounds which are the major constituents of CACE and CFACs (based on GC–MS analysis) [43]. The antioxidant activity of CACE and CFACs could be attributed to the presence of aromatic ring and hydroxyl groups can act as electron or hydrogen donators and neutralize the free radicals and reactive oxygen species [44].

3.2 Chemical composition analysis

Results from the GC–MS analysis of CACE and CFAC 1–3 are as summarized in Table 2. CACE consisted of phenol and derivatives (69.47%) followed by ketones (12.57%), alkanes (10.14%), acids (6.17%), furans and pyrans (4.44%), and benzene (1.70%). Phenol and derivatives as major constituents of AC were also reported by other researchers [23, 39, 44]. High yield of phenol and derivatives can be attributed to the high amount of lignin content (48.52 ± 0.63 wt%) in PKS [45].

After fractionation, a number of chemical compounds identified in the combined fractions (CFACs) were reduced compared to the CACE (41 compounds). About 15 chemical compounds were identified from GC–MS analysis on CFAC 1 where phenol and derivatives represented as its major compound group (98.52%), followed by furan (0.81%) and benzenes (0.67). The main phenols and derivatives compounds in CFAC 1 included phenol (34.41%), creosol (13.69%), phenol, 4-ethyl-2-methoxy- (ethylguaiacol, 12.29%), and phenol, 2-methoxy- (guaiacol, 10.74%). Other compounds were also identified including 2-furancarboxaldehyde (0.81%) and benzene (0.67%). In CFAC 2, 13 chemical compounds were identified with phenol and derivatives as its major compound group (95.93%), followed by ketones (4.07%). The main phenols and derivatives compounds in CFAC 2 were mainly 1,2-benzenediol (catechol, 20.42%), followed by 1,2-benzenediol, 3-methoxy- (3-methoxy catechol, 15.47%), methylparaben (13.49%), 1,2-benzenediol, 4-methyl- (4,methylcatechol, 9.20%), and vanillin (6.27%). Six chemical compounds were detected from GC–MS analysis of CFAC 3 with phenol and derivatives represented the major compound group (93.21%). This group is made up mainly of phenol, 2,6-dimethoxy-, known as syringol (46.09%) and 3,5-dimethoxy-4-hydroxytoluene (40.83%), followed by 6.29% of 1,2-benzenediol, 3-methylbenzenes.

The GC–MS analysis of the three combined fractions showed that all three were mainly made up of phenol and derivatives as the major compounds. In the CFAC 1, phenol which was the main chemical compound present in CACE was completely eluted in fractions 10 and 11. These

Table 2 Chemical profiles of CACE and CFAC 1–3 based on GC–MS analysis

No	Compound	Retention time (min)	Relative content (%)			
			CACE	CFAC 1	CFAC 2	CFAC 3
	Phenol and derivatives		64.97			
1	Phenol	6.203	40.72	34.41		
2	Phenol, 2-methyl-	7.423	2.24	3.75		
3	Phenol, 3-methyl-	7.754	2.17			
4	Phenol, 4-methyl- (*p*-cresol)	7.751		5.81		
5	Phenol, 2-methoxy- (guaiacol)	8.012	4.97			
6	Phenol, 2,6-dimethyl-	8.278		0.86		
7	Phenol, 2-ethyl-	8.745		0.93		
8	Phenol, 3,5-dimethyl-	8.908		1.98		
9	Phenol, 4-ethyl-	9.189		2.54		
10	Creosol	9.612	5.16	13.69		
11	1,2-Benzenediol (Catechol)	9.633			20.42	
12	Phenol, 2,3,6-trimethyl-	10.540		1.62		
13	1,2-Benzenediol, 3-methyl-	10.561				6.29
14	1,2-Benzenediol, 3-methoxy-	10.602			15.47	
15	Phenol, 4-ethyl-2-methoxy-	10.868	4.38	12.29		
16	1,2-Benzenediol, 4-methyl-	10.962			9.20	
17	Phenol, 2,6-dimethoxy- (syringol)	11.855	5.31		7.70	46.09
18	Eugenol	11.956		1.98		
19	Phenol, 3,4-dimethoxy-	11.982			4.09	
20	Phenol, 2-methoxy-4-propyl-	12.085		5.30		
21	1,3-Benzenediol, 4-ethyl-	12.255			3.84	
22	Vanillin	12.505			6.27	
22	Benzene, 1,2,3-trimethoxy-5-methyl-	12.536		2.62		
23	3,5-Dimethoxy-4-hydroxytoluene	13.099				40.83
24	Methylparaben	13.170			13.49	
	Furan and pyran		4.44			
1	Furfural	3.802	2.63			
2	2-Furancarboxaldehyde, 5-methyl-	5.943	1.81	0.81		
	Ketone		12.57			
1	2-Cyclopenten-1-one, 2-hydroxy-3-methyl-	6.955			2.63	
2	Benzaldehyde, 4-ethoxy-3-hydroxy-	12.083	1.35			
3	Apocynin	13.626			6.09	
4	Benzaldehyde, 3,4-dimethoxy-, methylmonoacetal	13.904	0.72			

Table 2 (continued)

No	Compound		Retention time (min)	Relative content (%)			
				CACE	CFAC 1	CFAC 2	CFAC 3
5	Ethanone, 1-(2,6-dihydroxy-4-methoxyphenyl)-	14.097		4.14			
6	Ethanone, 1-(4,5-diethyl-2-methyl-1-cyclopenten-1-yl)-	14.795					2.95
7	Ethanone, 1,1′-(6-methoxy-2,5-benzofurandiyl)bis-	15.336		0.74			
8	1-Butanone, 3-methyl-1-(2,4,6-trihydroxy-3-methylphenyl)-	16.901					2.04
9	2-Pentanone, 1-(2,4,6-trihydroxyphenyl)	16.904		2.27			
10	7,9-Di-tert-butyl-1-oxaspiro(4,5)deca-6,9-diene-2,8-dione	18.425		3.35	1.44		1.79
	Alkane			10.15			
1	Decane	6.514		3.12			
2	Cyclohexasiloxane, dodecamethyl-	11.482		2.28			
3	Cycloheptasiloxane, tetradecamethyl-	13.711		3.93			
4	Octasiloxane, 1,1,3,3,5,5,7,7,9,9,11,11,13,13,15,15-hexadecamethyl-	18.979		0.82			
	Acid			6.17			
1	Vanillic acid	13.106		5.00			
2	2,5-Dihydroxybenzoic acid	15.707		1.17			
	Benzene			1.70			
1	Benzene, propoxy-	7.547			0.67		
2	Benzene, 1-ethyl-3-(phenylmethyl)-	15.093		1.70			

compounds have similar polarity as their polarity was mainly attributed to the presence of 1 hydroxyl group (-OH). Presence of benzene compounds might be the remaining hydrocarbon content that had not been fully removed using solvent system of 100% *n*-hexane. Most of the hydrocarbons were removed when non-polar *n*-hexane was used as solvent system [31]. When the 9:1 solvent system of *n*-hexane:ethyl acetate, most phenols and derivatives were eluted in fractions 10 and 11. The dielectric constant of this solvent system was similar to toluene which was used by Wang et al. to remove most of phenol and its derivatives [31].

The ATR-FTIR spectra (within the 650 cm^{-1} to 4000 cm^{-1} wavenumber region) of the CACE and CFAC 1–3 are given in Fig. 1. The FTIR results corroborate the result obtained by GC–MS where the main chemical species present in CACE and CFACs used in this work are aromatic compounds, carbonylic, phenolic, and carboxylic acids. The peak at 3600–3200 cm^{-1} and 1360 cm^{-1} corresponds to the O–H stretching and O–H bending vibration, respectively, which confirms the appearance of alcohols and phenols [46, 47]. The spectrum also showed that the band of C–H stretching with wave number of 3000–2800 cm^{-1} indicates the present of alkanes groups in the pyroligneous (Islam et al., 2003; Tsai et al., 2007). Furthermore, the peak at 2820–2960 cm^{-1} is strengthened, which may be caused by the C–H stretching vibration of aromatic compounds. The peak in the range of 1700–1725 cm^{-1} corresponds to C = O stretching group, representing the presence of carboxylic acid, phenol, ketone, aldehyde functional groups [46, 47]. The peaks at 1600 cm^{-1} and 1500 cm^{-1} were assigned to aromatic C = C–C stretch which implies the aromatic structure while 670–850 cm^{-1} corresponded to C–H bending which can be observed in aromatic structure. The higher peak intensity at 1270–1230 cm^{-1} was observed in CFAC 3 which is due to the aryl-O-C stretch in aromatic ethers [47]. The intensity of C-O stretch around 1100–1200 cm^{-1} represented ether and aromatic compounds. These peaks were observed to have higher intensity for CFAC 2 which is due to the presence of two hydroxyl group in catechol derivatives and methoxy group in syringol derivatives [48].

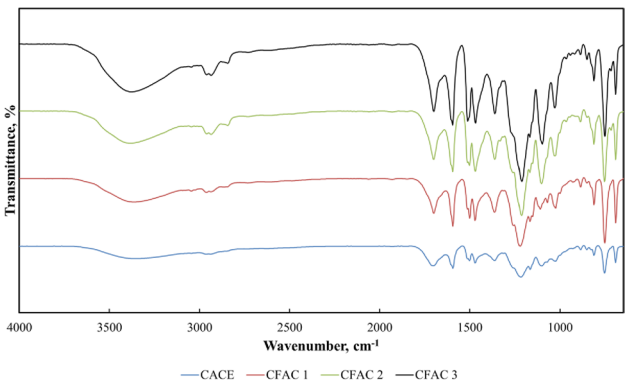

Fig. 1 ATR-FTIR spectra of the CACE and CFAC 1–3 in the spectral range from 650 to 4000 cm^{-1}

3.3 Antibacterial activity

Figure 2 shows that CACE and CFAC exhibited antibacterial activity against all strains tested. For 30 µg of kanamycin, bacterial strains are regarded towards antibacterial agent as resistant when diameter is less than or equal to 13 mm, intermediate when diameter is in between 14 and 17 mm, and sensitive/susceptible when the diameter is more than 17 mm [49]. *S. aureus* was shown to be susceptible against CACE and CFACs with the smallest and biggest inhibition zone demonstrated by CFAC 1 (25.2 ± 0.3 mm, $p < 0.0001$) and CFAC 3 (48.8 ± 0.8 mm, $p < 0.0001$), respectively. *P. aeruginosa* was susceptible towards CACE, CFAC 2, and CFAC 3 but intermediately susceptible towards CFAC 1. *E. faecalis* was susceptible towards CFAC 2 and CFAC 3, less susceptible to CACE (16.2 ± 0.8 mm) but resistant to CFAC 1 (9.8 ± 0.6 mm). *E. coli* was susceptible only to CFAC 3 and less susceptible to the others.

Table 3 shows the MIC and MBC values of CACE and CFAC 1–3 against pathogenic bacteria *S. aureus*, *E. faecalis*, *P. aeruginosa*, and *E. coli*. Treatment of CACE and CFACs has significant inhibitory effect ($p < 0.0001$) on the growth of all tested bacterial strains. *S. aureus* was the most susceptible to the sample treatment as MIC recorded was the lowest as compared towards other bacterial strains for CACE, CFAC 1, CFAC 2, and CFAC 3 with 0.78 ± 0.00 mg/mL, 0.33 ± 0.11 mg/mL, 0.16 ± 0.06 mg/mL, and 0.10 ± 0.00 mg/mL. The MBC values of the samples against *all bacterial strains* were similar to MIC except for CFAC 1 which MBC (3.13 ± 0.00 mg/mL) was doubled the concentration of MIC

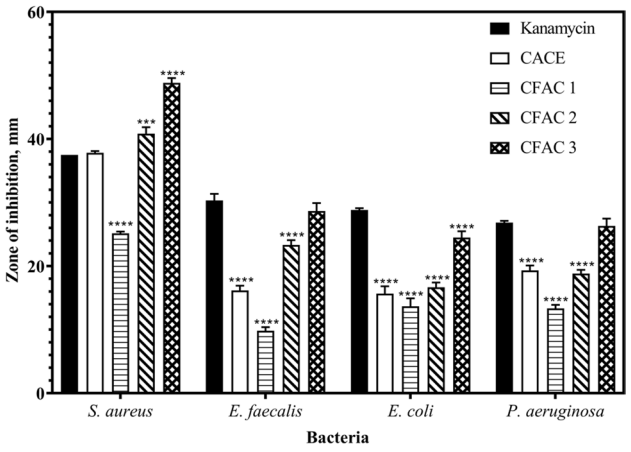

Fig. 2 Diameter of inhibition zone of CACE and combined fractions (CFACs) towards *E. coli*. *P. aeruginosa*, *S. aureus*, and *E. faecalis* (*** represents $p < 0.001$ and **** represents $p < 0.0001$)

Table 3 Minimum inhibition concentration (MIC) and minimum bactericidal concentration (MBC) of CACE and CFAC 1–3 against pathogenic bacterial strains of *S. aureus*, *E. faecalis*, *P. aeruginosa*, and *E. coli*

Strain	MIC (mg/mL)				MBC (mg/mL)			
	CACE	CFAC 1	CFAC 2	CFAC 3	CACE	CFAC 1	CFAC 2	CFAC 3
E. coli	3.13 ± 0.00	1.56 ± 0.00	3.13 ± 0.00	1.56 ± 0.00	3.13 ± 0.00	3.13 ± 0.00	3.13 ± 0.00	1.56 ± 0.00
P. aeruginosa	1.56 ± 0.00	1.56 ± 0.00	3.13 ± 0.00	0.78 ± 0.00	1.56 ± 0.00	1.56 ± 0.00	3.13 ± 0.00	0.78 ± 0.00
S. aureus	0.78 ± 0.00	0.33 ± 0.11	0.16 ± 0.06	0.10 ± 0.00	0.78 ± 0.00	3.13 ± 0.00	0.33 ± 0.11	0.13 ± 0.06
E. faecalis	0.78 ± 0.00	1.56 ± 0.00	0.78 ± 0.00	0.39 ± 0.00	1.04 ± 0.45	3.13 ± 0.00	0.78 ± 0.00	0.39 ± 0.00

(1.56 ± 0.00 mg/mL) against *E. coli* and *E. faecalis*, and eight time bigger than MIC (0.33 ± 0.11 mg/mL) against *S. aureus*. These showed that CACE, CFAC2, and CFAC 3 have bactericidal effect against these bacterial strains. These results were better than the MBC reported by Ariffin et al. [50] as the MBC of *E. coli* was 62.5 mg/mL while MBCs of *P. aeruginosa*, *S. aureus*, and *B. subtilis* were 125 mg/mL. The order of bacterial cell susceptibility/sensitivity based on MIC and MBC values in the descending order is as follows: *S. aureus* > *E. faecalis* > *P. aeruginosa* > *E. coli*.

CACE and CFACs demonstrated strongest antibacterial effect on *S. aureus* activity. *E. faecalis* showed less susceptibility due to its resistance to phenolic compounds [51]. Overall, MIC and MBC values of CACE and CFACs against gram-positive bacteria *S. aureus* and *E. faecalis* were lower compared to gram-negative bacteria *E. coli* and *P. aeruginosa*. These results revealed that gram-positive bacteria were more susceptible to the CACE and CFACs than gram-negative bacteria which could be due to the absence of outer membrane on the gram-positive bacteria [39]. The outer membrane which includes the asymmetric distribution of the lipids with phospholipids and lipopolysaccharide (LPS) located in the inner and outer leaflets, respectively, can act as a barrier to many environmental substances including antibiotics [52]. Many reports agreed that further refining of AC has lowered the MIC value. The MIC value of AC has been reported to decrease by more than half when AC was concentrated and extracted using dichloromethane [52]. Antibacterial activity of the CACE and CFACs was attributed to the combination of many phenolic compounds which are present in the AC. A study also has suggested that chemical compounds in AC exhibited synergistic effect on its antibacterial activity [39]. The site(s) and number of hydroxyl groups on the phenol group are correlated to increase in toxicity to microorganism [53]. This could be the reason for better MIC and MBC of CFAC 2 and CFAC 3 as compared to CFAC 1 as formers have catechol compounds, as reported in GC–MS analysis, which was absence in the CFAC 1. The mechanisms thought to be responsible for phenolic toxicity to microorganisms include enzyme inhibition by the oxidized compounds, possibly through reaction with sulfhydryl groups or through more nonspecific interactions with the proteins [53]. Eugenol is was reported to act as antibacterial agent by disrupting cell membrane [54]. It works by increasing nonspecific permeability of cell membrane causing leakage of ions and cellular contents thus leading to death. Phenolic compounds such as eugenol also act by inhibiting the bacterial DNA and protein synthesis [55, 56].

3.4 Molecular docking

Molecular docking on CFAC 3 compounds was performed using AutoDock Vina to predict their antibacterial mode of action towards DNA synthesis inhibition through DNA inhibition and DNA gyrase inhibition and protein synthesis inhibition through tyrosyl-tRNA synthetase inhibition. The lowest binding energy, hydrogen bond (H bond), and π interactions of each compound and the active site of the receptors are shown in Table 4. According to the obtained docking results, all CFAC 3 compounds formed stable ligand–protein-complex with target enzymes indicated by its negative value binding energy.

The ATPase activity provides energy for the DNA supercoiling by DNA gyrase during bacterial DNA replication cycle [28]. The docking setup was first validated by performing self-docking of the ligand crystal in the ATPase activity site. The result of self-docking validation reproduced the same binding mode as experimental ligand crystal towards DNA gyrase with a small root mean square deviation (RMSD) of 0.524 Å. The docked ligand crystal revealed the important interaction of Thr164 towards water molecule as reported by Brvar et al. [57]. The CFAC 3 compounds have successfully bound to the ATPase activity site of bacterial DNA gyrase B with binding energy within the range of − 5.4 kcal/mol to − 6.9 kcal/mol. 1-Butanone, 3-methyl-1-(2,4,6-trihydroxy-3-methylphenyl)- compound was the most stable ligand (binding energy of − 6.9 kcal/mol) as shown in Fig. 3a. The binding energy of the CFAC 3 compounds were higher than the crystal ligand (− 7.9 kcal/mol) because the CFAC 3 compounds formed maximum of three hydrogen bonds compared to five hydrogen bonds formed by the crystal ligand within the active site. For bacterial DNA gyrase B, the CFAC 3 compounds displayed similar binding mode by occupying the pocket which interacts with the key

Table 4 Binding interaction of CFAC 3 compounds towards DNA gyrase (4DUH), and tyrosyl-tRNA synthetase (1JIJ), respectively

Ligands	DNA gyrase 4DUH			Tyrosyl-tRNA synthetase 1JIJ		
	Binding energy (kcal/mol)	H bond	π bond	Binding energy (kcal/mol)	H bond	π bond
Crystal ligand*	−7.9	Asn46, Asp73, Arg76, Gly101, Arg136	Ile78, Pro79, Ile94	−7.9	Tyr36, Cys37, Gly38, Asp40, Gly49, His50, Asp80, Tyr170, Asp177, Gly193, Asp195	Leu70
Syringol	−5.4	Thr165	Asn46, Glu50, Ile78	−5.7	Tyr170	-
3-Methylcatechol	−5.8	Asp73, Gly77, Thr165	Asn46, Glu50, Ile78, Pro79, Lyus103	−6.3	Thr75, Asn124, Tyr170, Asp177	Leu70
3,5-Dimethoxy-4-hydroxytoluene	−5.9	Thr165	Glu50, Arg76, Ile78, Pro79, Lys103	−6.3	Asp40, Thr75, Tyr170	Cys37, Leu70
Ethanone, 1-(4,5-diethyl-2-methyl-1-cyclopenten-1-yl)-	−5.8	Asn46, Lys103	Val43, Val71	−5.3	Gly193, Gln196	His50, Pro53, Phe54,
1-Butanone, 3-methyl-1-(2,4,6-trihydroxy-3-methylphenyl)-	−6.9	Asp73, Thr165	Val43, Glu50, Lys103, Val120	−7.5	Tyr36, Tyr170,Gln174	Leu70
7,9-Di-tert-butyl-1-oxaspiro(4,5) deca-6,9-diene-2,8-dione	−5.3	-	Pro79, Ile94, Lys103,	−7.3	Asp40	Tyr36, Cys37, Leu70, Tyr170, Ile200

*4′-methyl-N(2)-phenyl-[4,5′-bithiazole]-2,2′-diamine (DNA gyrase 4DUH) and SB-219383 (tyrosyl-tRNA synthetase 1JIJ)

amino acids Asp73 and Gly77 [28]. Besides that, the CFAC 3 compounds insert into a hydrophobic pocket located at the bottom of ATP adenosine binding pocket which are made up of residues Ile78, Ala91, Ile94, Met95, Val120, Leu132, Ile134, Thr165, and Val167 [58]. These results corroborate ability of these compounds to inhibit DNA synthesis through binding with bacterial DNA gyrase.

Tyrosyl-tRNA plays an important role in the protein synthesis. Redocking of the crystal ligand (SB-219383) showed small variation compared to the experimental crystal ligand with RMSD of 1.871 Å. RMSD values between 1 Å and 2 Å is acceptable to show a conserved binding pattern as the experimental crystal ligand [59]. Docking results of selected CFAC 3 compounds against tyrosyl-tRNA synthetase indicated a similar conserved binding region to the SB-219383 with binding energy range between −5.3 kcal/mol and 7.5 kcal/mol. The lowest binding energy was found for compound 1-butanone, 3-methyl-1-(2,4,6-trihydroxy-3-methylphenyl)- (−7.5 kcal/mol, Fig. 3b), followed by 7,9-di-tert-butyl-1-oxaspiro(4,5)deca-6,9-diene-2,8-dione (−7.3 kcal/mol), 3-methylcatechol (−6.3 kcal/mol), and 3,5-dimethoxy-4-hydroxytoluene (−6.3 kcal/mol). Most of the compounds formed hydrogen binding to Tyr170 and Thr75, and Π-Π bond with Leu70. The binding residues of the tyrosyl-tRNA synthetase active site are highly conserved among several bacteria including *S. aureus* (Tyr36, Asp177, Gln174, Gln196, Tyr170, and Asp80) and *E. coli* (Tyr37, Asp182, Gln179, Gln201, Tyr175, and Asp81). Asp40 also forms a hydrogen bond with the carboxyl oxygen of tyrosine [60]. Gly193 of *S. aureus* TyrRS also forms the same hydrogen bond with the 2′-OH of the ribosyl moiety of tyrosyl adenylate [17]. Xiao et al. has reported the hydrophobic interaction of aniline moiety towards the strong hydrophobic residue Leu70 [61].

In terms of structure–activity relationship, chemical compounds with more hydroxyl groups exhibited lower binding energy to the enzymes [62]. 1-Butanone, 3-methyl-1-(2,4,6-trihydroxy-3-methylphenyl)- which has three hydroxyl groups exhibited the lowest binding energy towards both bacterial DNA gyrase (−6.9 kcal/mol) and tyrosyl-tRNA synthetase (−7.5 kcal/mol), followed by 3-methyl catechol with two hydroxyl groups and syringol with one hydroxyl groups. Increase in the number of methyl or alkyl groups has also shown in lower binding energy as observed in additional of a methyl group in 3,5-dimethoxy-4-hydroxytoluene and a methyl and a butanone chain in 1-butanone, 3-methyl-1-(2,4,6-trihydroxy-3-methylphenyl)- compared to syringol [63]. The additional of these groups cause an increase hydrophobic interaction with the non-polar amino acids on the receptors [62, 63]. These molecular docking results show

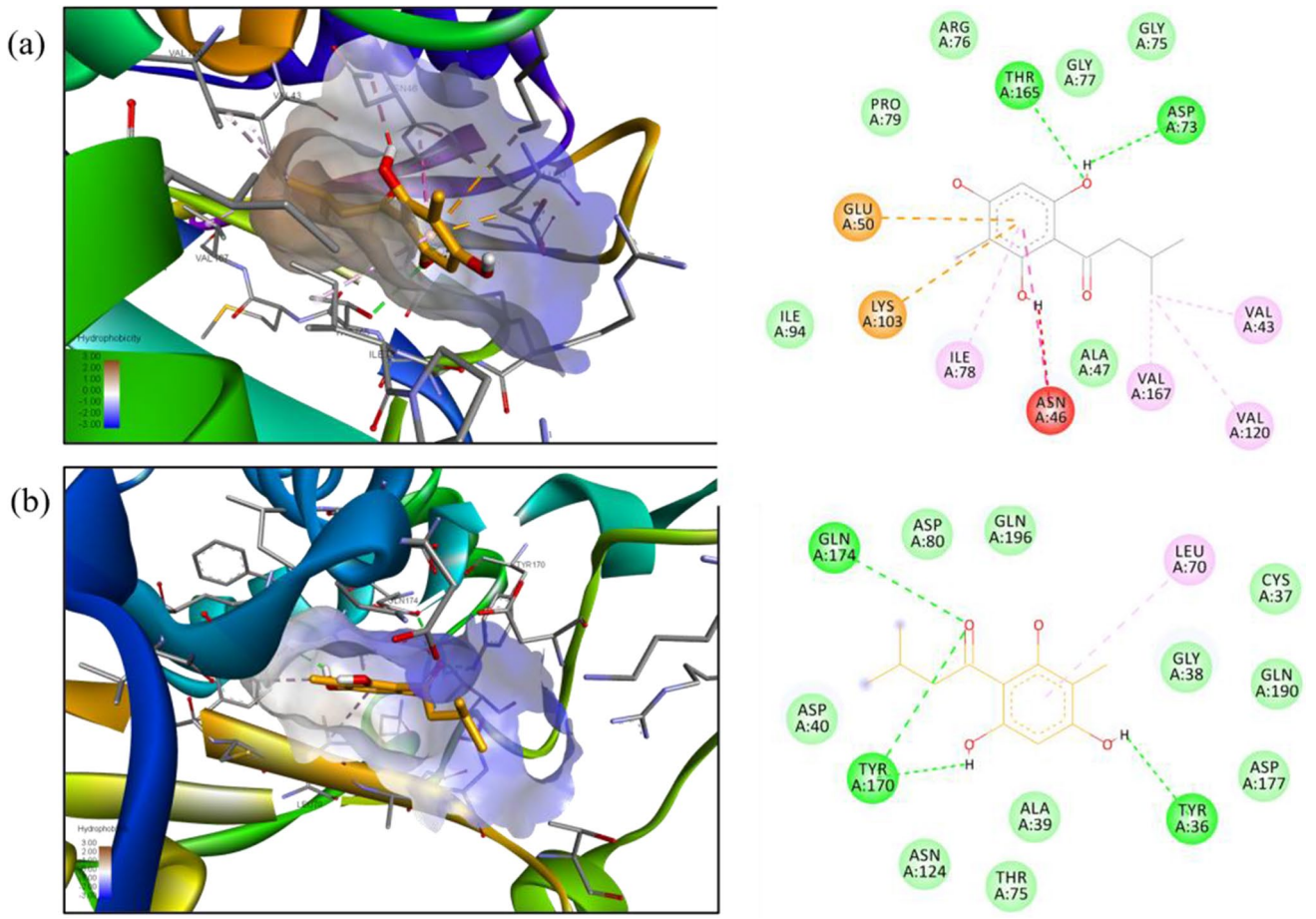

Fig. 3 3D and 2D interaction of **a** 1-butanone, 3-methyl-1-(2,4,6-trihydroxy-3-methylphenyl)- towards DNA gyrase (4DUH) and **b** 1-butanone, 3-methyl-1-(2,4,6-trihydroxy-3-methylphenyl)- towards tyrosyl-tRNA synthase (1JIJ)

CFAC 3 compounds can be an alternative as antibacterial agents for antiseptic application with their multi-pronged modes of antibacterial action towards several bacterial enzymes, though, experimental study needs to be carried out to further validate the proposed mechanisms.

4 Conclusion

CFAC 1–3 have exhibited at least similar or higher high antioxidant activity and antibacterial activity as compared to the CACE which are associated to the presence of many phenolic compounds and its derivatives based on the analysis of GC–MS. It exhibited both antibacterial activity against pathogenic *E. coli*, *P. aeruginosa*, *S. aureus*, and *E. faecalis*. Molecular docking analysis suggested favorable binding energy for all chemical compounds present in CFAC 3 notably 1-butanone, 3-methyl-1-(2,4,6-trihydroxy-3-methylphenyl)- towards DNA gyrase, and tyrosyl-tRNA synthetase. This further suggested that CFAC 3 compounds might have multiple targets or possess a nonspecific mode of antibacterial action which can be proven and validated experimentally.

Funding The authors acknowledged the financial assistance from Universiti Teknologi Malaysia for the Research University Grant (07G78). We would also like to express our gratitude to UTM Digital Centre for the high-performance computing facilities.

Data availability Not applicable.

Code availability Not applicable.

Declarations

Ethics approval Not applicable.

Consent to participate All authors have given consent to participate.

Consent for publication All authors have provided consent for publication.

Conflict of interest The authors declare no competing interests.

References

1. Malaysian-German Chamber of Commerce and Industry (2017) Oil palm biomass & biogas In Malaysia, 2017. EU-Malaysia Chamb. Commer. Ind. Retrieved from www.malaysia.ahk.de
2. Ahmad R, Hamidin N, Ali UFM, Abidin CZA (2015) Characterization of bio-oil from palm kernel shell pyrolysis. J Mech Eng Sci 7:1134–1140. https://doi.org/10.15282/jmes.7.2014.12.0110
3. Mathew S, Zakaria ZA (2015) Pyroligneous acid—the smoky acidic liquid from plant biomass. Appl Microbiol Biotechnol 99:611–622. https://doi.org/10.1007/s00253-014-6242-1
4. Abnisa F, Daud WMAW, Husin WNW, Sahu JN (2011) Utilization possibilities of palm shell as a source of biomass energy in Malaysia by producing bio-oil in pyrolysis process. Biomass Bioenerg 35:1863–1872. https://doi.org/10.1016/J.BIOMBIOE.2011.01.033
5. Ma C, Song K, Yu J et al (2013) Pyrolysis process and antioxidant activity of pyroligneous acid from Rosmarinus officinalis leaves. J Anal Appl Pyrolysis 104:38–47. https://doi.org/10.1016/j.jaap.2013.09.011
6. Clark M, Tilman D (2017) Comparative analysis of environmental impacts of agricultural production systems, agricultural input efficiency, and food choice. Environ Res Lett 12:064016. https://doi.org/10.1088/1748-9326/aa6cd5
7. Punjataewakupt A, Napavichayanun S, Aramwit P (2019) The downside of antimicrobial agents for wound healing. Eur J Clin Microbiol Infect Dis 38:39–54
8. Ugwah-Oguejiofor CJ, Okoli CO, Ugwah MO et al (2019) Acute and sub-acute toxicity of aqueous extract of aerial parts of Caralluma dalzielii N. E. Brown in mice and rats. Heliyon 5:e01179. https://doi.org/10.1016/j.heliyon.2019.e01179
9. Araújo E de S, Pimenta AS, Feijó FMC et al (2018) Antibacterial and antifungal activities of pyroligneous acid from wood of Eucalyptus urograndis and Mimosa tenuiflora. J Appl Microbiol 124:85–96. https://doi.org/10.1111/jam.13626
10. Rabiu Z, Hamzah MAAM, Hasham R, Zakaria ZA (2020) Characterization and antiinflammatory properties of fractionated pyroligneous acid from palm kernel shell. Environ Sci Pollut Res 1–9.https://doi.org/10.1007/s11356-020-09209-x
11. Aguirre JL, Baena J, Martín MT et al (2020) Composition, ageing and herbicidal properties of wood vinegar obtained through fast biomass pyrolysis. Energies 13:2418. https://doi.org/10.3390/en13102418
12. Suresh G, Pakdel H, Rouissi T et al (2020) Evaluation of pyroligneous acid as a therapeutic agent against Salmonella in a simulated gastrointestinal tract of poultry. Braz J Microbiol 51:1309–1316. https://doi.org/10.1007/s42770-020-00294-1
13. Kimura Y, Suto S, Tatsuka M (2002) Evaluation of carcinogenic/co-carcinogenic activity of chikusaku-eki, a bamboo charcoal by-product used as a folk remedy, in BALB/c 3T3 cells. Biol Pharm Bull 25:1026–1029. https://doi.org/10.1248/bpb.25.1026
14. Tiilikkala K, Fagernäs L, Tiilikkala J (2014) History and use of wood pyrolysis liquids as biocide and plant protection product. Open Agric J 4:111–118. https://doi.org/10.2174/1874331501004010111
15. Miladi H, Zmantar T, Chaabouni Y et al (2016) Antibacterial and efflux pump inhibitors of thymol and carvacrol against food-borne pathogens. Microb Pathog 99:95–100. https://doi.org/10.1016/j.micpath.2016.08.008
16. Nafisi S, Hajiakhoondi A, Yektadoost A (2004) Thymol and carvacrol binding to DNA: model for DRUG-DNA interaction. Biopolymers 74:345–351. https://doi.org/10.1002/bip.20080
17. Pisano MB, Kumar A, Medda R et al (2019) Antibacterial activity and molecular docking studies of a selected series of hydroxy-3-arylcoumarins. Molecules 24.https://doi.org/10.3390/molecules24152815
18. Meng X-Y, Zhang H-X, Mezei M, Cui M (2011) Molecular docking: a powerful approach for structure-based drug discovery. Curr Comput Aided Drug Des 7:146–157
19. Zulkifli SE, Hamzah MAAM, Yahayu M et al (2021) (2021) Optimisation of microwave-assisted production of acid condensate from palm kernel shell and its biological activities. Biomass Convers Biorefinery 1:1–11. https://doi.org/10.1007/S13399-021-01631-6
20. Ma C, Li W, Zu Y et al (2014) Antioxidant properties of pyroligneous acid obtained by thermochemical conversion of Schisandra chinensis baill. Molecules 19:20821–20838. https://doi.org/10.3390/molecules191220821
21. Brand-Williams W, Cuvelier ME, Berset C (1995) Use of a free radical method to evaluate antioxidant activity. LWT - Food Sci Technol 28:25–30. https://doi.org/10.1016/S0023-6438(95)80008-5
22. Re R, Pellegrini N, Proteggente A et al (1999) Antioxidant activity applying an improved ABTS radical cation decolorization assay. Free Radic Biol Med 26:1231–1237. https://doi.org/10.1016/S0891-5849(98)00315-3
23. Zhai M, Shi G, Wang Y et al (2015) Chemical compositions and biological activities of pyroligneous acids from walnut shell. BioResources 10:1715–1729. https://doi.org/10.15376/biores.10.1.1715-1729
24. Hudzicki J (2009) Kirby-Bauer disk diffusion susceptibility test protocol. Am Soc Microbiol. Retrieved from https://asm.org/Protocols/Kirby-Bauer-Disk-Diffusion-Susceptibility-Test-Pro
25. Abas FZ, Zakaria ZA, Ani FN (2018) Antimicrobial properties of optimized microwave-assisted pyroligneous acid from oil palm fiber. J Appl Pharm Sci 8:65–71. https://doi.org/10.7324/JAPS.2018.8711
26. Elshikh M, Ahmed S, Funston S et al (2016) Resazurin-based 96-well plate microdilution method for the determination of minimum inhibitory concentration of biosurfactants. Biotechnol Lett 38:1015–1019. https://doi.org/10.1007/s10529-016-2079-2
27. Trott O, Olson AJ (2010) AutoDock Vina: improving the speed and accuracy of docking with a new scoring function, efficient optimization, and multithreading. J Comput Chem 31:455–461. https://doi.org/10.1002/jcc.21334
28. Ghannam IAY, Abd El-Meguid EA, Ali IH et al (2019) Novel 2-arylbenzothiazole DNA gyrase inhibitors: synthesis, antimicrobial evaluation, QSAR and molecular docking studies. Bioorg Chem 93:103373. https://doi.org/10.1016/j.bioorg.2019.103373
29. Hatami T, Emami SA, Miraghaee SS, Mojarrab M (2014) Total phenolic contents and antioxidant activities of different extracts and fractions from the aerial parts of Artemisia biennis Willd. Iran J Pharm Res IJPR 13:551–559. https://doi.org/10.22037/ijpr.2014.1518
30. Ezealigo US, Joshua PE, Ononiwu CP et al (2020) Total phenolic and flavonoid content and in vitro antioxidant activity of methanol extract and solvent fractions of Desmodium ramosissimum G. Don. Med Sci Forum 2021 2:15. https://doi.org/10.3390/CAHD2020-08594
31. Wang S, Wang Y, Leng F et al (2016) Separation and enrichment of catechol and sugars from bio-oil aqueous phase. BioResources 11. https://doi.org/10.15376/biores.11.1.1707-1720
32. Jing L, Ma H, Fan P et al (2015) Antioxidant potential, total phenolic and total flavonoid contents of Rhododendron anthopogonoides and its protective effect on hypoxia-induced injury in PC12 cells. BMC Complement Altern Med 15:1–12. https://doi.org/10.1186/S12906-015-0820-3/FIGURES/5
33. Collard FX, Blin J (2014) A review on pyrolysis of biomass constituents: mechanisms and composition of the products obtained from the conversion of cellulose, hemicelluloses and lignin. Renew Sustain Energy Rev 38:594–608

34. Abas FZ, Ani FN, Zakaria ZA (2018) Microwave-assisted production of optimized pyrolysis liquid oil from oil palm fiber. J Clean Prod 182:404–413. https://doi.org/10.1016/j.jclepro.2018.02.052
35. Mathew S, Zakaria ZA, Musa NF (2015) Antioxidant property and chemical profile of pyroligneous acid from pineapple plant waste biomass. Process Biochem 50:1985–1992. https://doi.org/10.1016/j.procbio.2015.07.007
36. Aryal S, Baniya MK, Danekhu K et al (2019) Total phenolic content, flavonoid content and antioxidant potential of wild vegetables from Western Nepal. Plants 8.https://doi.org/10.3390/PLANTS8040096
37. Wei Q, Ma X, Zhao Z et al (2010) Antioxidant activities and chemical profiles of pyroligneous acids from walnut shell. J Anal Appl Pyrolysis 88:149–154. https://doi.org/10.1016/J.JAAP.2010.03.008
38. Kim SP, Yang JY, Kang MY et al (2011) Composition of liquid rice hull smoke and anti-inflammatory effects in mice. J Agric Food Chem 59:4570–4581. https://doi.org/10.1021/jf2003392
39. Yang JF, Yang CH, Liang MT et al (2016) Chemical composition, antioxidant, and antibacterial activity of wood vinegar from litchi chinensis. Molecules 21:1–10. https://doi.org/10.3390/molecules21091150
40. Craft BD, Kerrihard AL, Amarowicz R, Pegg RB (2012) Phenol-based antioxidants and the in vitro methods used for their assessment. Compr Rev Food Sci Food Saf 11:148–173. https://doi.org/10.1111/J.1541-4337.2011.00173.X
41. Liu X, Sun H, Gao P et al (2018) Antioxidant properties of compounds isolated from wood vinegar by activity-guided and pH-gradient extraction. J Wood Chem Technol 38:313–323. https://doi.org/10.1080/02773813.2018.1488873
42. Sekher Pannala A, Chan TS, O'Brien PJ, Rice-Evans CA (2001) Flavonoid B-ring chemistry and antioxidant activity: fast reaction kinetics. Biochem Biophys Res Commun 282:1161–1168. https://doi.org/10.1006/bbrc.2001.4705
43. Loo AY, Jain K, Darah I (2008) Antioxidant activity of compounds isolated from the pyroligneous acid, Rhizophora apiculata. Food Chem 107:1151–1160. https://doi.org/10.1016/j.foodchem.2007.09.044
44. Mahmud KN, Hashim NM, Ani FN, Zakaria ZA (2019) Antioxidants, toxicity, and nitric oxide inhibition properties of pyroligneous acid from palm kernel shell biomass. Waste and Biomass Valorization 1–13.https://doi.org/10.1007/s12649-019-00857-w
45. Wang S, Wang K, Liu Q et al (2009) Comparison of the pyrolysis behavior of lignins from different tree species. Biotechnol Adv 27:562–567. https://doi.org/10.1016/j.biotechadv.2009.04.010
46. Zheng H, Wang R, Zhang Q et al (2020) Pyroligneous acid mitigated dissemination of antibiotic resistance genes in soil. Environ Int 145:106158. https://doi.org/10.1016/J.ENVINT.2020.106158
47. Coates J (2006) Interpretation of infrared spectra, a practical approach. Encycl Anal Chem. https://doi.org/10.1002/9780470027318.A5606
48. Mahmud KN, Yahayu M, Sarip SHM et al (2016) Evaluation on efficiency of pyroligneous acid from palm kernel shell as antifungal and solid pineapple biomass as antibacterial and plant growth promoter. Sains Malaysiana 45:1423–1434
49. Pengov A, Ceru S (2003) Antimicrobial drug susceptibility of Staphylococcus aureus strains isolated from bovine and ovine mammary glands. J Dairy Sci 86:3157–3163. https://doi.org/10.3168/jds.S0022-0302(03)73917-4
50. Ariffin SJ, Yahayu M, El-Enshasy H et al (2017) Optimization of pyroligneous acid production from palm kernel shell and its potential antibacterial and antibiofilm activities. Indian J Exp Biol 55:427–435
51. Gutiérrez-Fernández J, García-Armesto M, Álvarez-Alonso R et al (2013) Antimicrobial activity of binary combinations of natural and synthetic phenolic antioxidants against Enterococcus faecalis. J Dairy Sci 96:4912–4920. https://doi.org/10.3168/jds.2013-6643
52. Ibrahim D, Kassim J, Lim S et al (2014) Evaluation of antibacterial effects of Rhizophora apiculata pyroligneous acid on pathogenic bacteria. Malays J Microbiol Pathog Bact 10:197–204
53. Cowan MM (1999) Plant products as antimicrobial agents. Clin Microbiol Rev 12:564–582. https://doi.org/10.1128/cmr.12.4.564
54. Devi KP, Nisha SA, Sakthivel R, Pandian SK (2010) Eugenol (an essential oil of clove) acts as an antibacterial agent against Salmonella typhi by disrupting the cellular membrane. J Ethnopharmacol 130:107–115. https://doi.org/10.1016/j.jep.2010.04.025
55. Xu JG, Liu T, Hu QP, Cao XM (2016) Chemical composition, antibacterial properties and mechanism of action of essential oil from clove buds against staphylococcus aureus. Molecules 21.https://doi.org/10.3390/molecules21091194
56. Niu D, Wang QY, Ren EF et al (2019) Multi-target antibacterial mechanism of eugenol and its combined inactivation with pulsed electric fields in a hurdle strategy on Escherichia coli. Food Control 106:106742. https://doi.org/10.1016/j.foodcont.2019.106742
57. Brvar M, Perdih A, Renko M et al (2012) Structure-based discovery of substituted 4,5′-bithiazoles as novel DNA gyrase inhibitors. J Med Chem 55:6413–6426
58. Huang X, Guo J, Liu Q et al (2018) Identification of an auxiliary druggable pocket in the DNA gyrase ATPase domain using fragment probes. Medchemcomm 9:1619–1629. https://doi.org/10.1039/C8MD00148K
59. Qiu X, Janson CA, Smith WW et al (2001) Crystal structure of Staphylococcus aureus tyrosyl-tRNA synthetase in complex with a class of potent and specific inhibitors. Protein Sci 10:2008–2016. https://doi.org/10.1110/ps.18001
60. Li T, Froeyen M, Herdewijn P (2008) Comparative structural dynamics of Tyrosyl-tRNA synthetase complexed with different substrates explored by molecular dynamics. Eur Biophys J 38:25–35. https://doi.org/10.1007/s00249-008-0350-8
61. Xiao ZP, Ma TW, Liao ML et al (2011) Tyrosyl-tRNA synthetase inhibitors as antibacterial agents: synthesis, molecular docking and structure-activity relationship analysis of 3-aryl-4-arylaminofuran-2(5H)-ones. Eur J Med Chem 46:4904–4914. https://doi.org/10.1016/j.ejmech.2011.07.047
62. Khodarahmi G, Asadi P, Farrokhpour H et al (2015) Design of novel potential aromatase inhibitors via hybrid pharmacophore approach: docking improvement using the QM/MM method. RSC Adv 5:58055–58064. https://doi.org/10.1039/C5RA10097F
63. Leung CS, Leung SSF, Tirado-Rives J, Jorgensen WL (2012) Methyl effects on protein–ligand binding. J Med Chem 55:4489. https://doi.org/10.1021/JM3003697